

Effect of Pleistocene Climatic Oscillations on the Phylogeography and Demography of Red Knobby Newt (*Tylototriton shanjing*) from Southwestern China

Guohua Yu^{1,2,3}, Mingwang Zhang^{1,3*}, Dingqi Rao^{1*}, Junxing Yang^{1*}

1 State Key Laboratory of Genetic Resources and Evolution, Kunming Institute of Zoology, Chinese Academy of Sciences, Kunming, Yunnan, China, **2** University of Chinese Academy of Sciences, Beijing, China, **3** College of Animal Science and Technology, Sichuan Agricultural University, Ya'an, Sichuan, China

Abstract

Factors that determine the genetic structure of species in southwestern China remain largely unknown. In this study, phylogeography and demography of *Tylototriton shanjing* was investigated from a mitochondrial perspective to address the role of the Quaternary ice ages in shaping phylogeographic history and genetic diversity of Yunnan. A total of 146 individuals from 19 populations across the entire range of the species were collected. We detected four maternal phylogenetic lineages corresponding to four population groups, and found that major glaciation events during the Pleistocene have triggered the intra-specific divergence. Coalescent simulations indicated that the populations retreated to different refugia located in southern Yunnan, northwestern Yunnan, the border region of western Yunnan with Myanmar, and middle-western Yunnan, respectively, during previous glacial periods in the Pleistocene, and these four refugia were not retained during the Last Glacial Maximum. Population expansions occurred during the last inter-glaciation, during which ice core and pollen data indicated that the temperature and precipitation gradually increased, and declines of population sizes started after the beginning of the Last Glacial Maximum when the climate became cooler and dryer. The paleo-drainage system had no contribution to the current genetic structure and the rivers were not dispersal barriers for this salamander.

Citation: Yu G, Zhang M, Rao D, Yang J (2013) Effect of Pleistocene Climatic Oscillations on the Phylogeography and Demography of Red Knobby Newt (*Tylototriton shanjing*) from Southwestern China. PLoS ONE 8(2): e56066. doi:10.1371/journal.pone.0056066

Editor: Daniele Canestrelli, Tuscia University, Italy

Received: October 20, 2012; **Accepted:** January 4, 2013; **Published:** February 12, 2013

Copyright: © 2013 Yu et al. This is an open-access article distributed under the terms of the Creative Commons Attribution License, which permits unrestricted use, distribution, and reproduction in any medium, provided the original author and source are credited.

Funding: This study was supported by the open funds of the State Key Laboratory of Genetic Resource and Evolution, Kunming Institute of Zoology, the Chinese Academy of Sciences (GREKF11–01) and Shuang Zhi Ji Hua Foundation of Sichuan Agricultural University (01570709). The funders had no role in study design, data collection and analysis, decision to publish, or preparation of the manuscript.

Competing Interests: The authors have declared that no competing interests exist.

* E-mail: raodq@mail.kiz.ac.cn (DR); yangjx@mail.kiz.ac.cn (JY); mwzhangkiz@hotmail.com (MZ)

☯ These authors contributed equally to this work.

Introduction

Quaternary climatic oscillations had profound effects on the geographical distribution and genetic structure of many species. Population genetic analyses have shown that during the Pleistocene, many floral and faunal species in the Northern Hemisphere migrated southward and survived in refugia during glacial periods and subsequently expanded northward from southern refugia during interglacial periods [1]. China is an important global Pleistocene refugia [2]. The Kunlun-Huanghe Movements (1.1–0.6 Mya) uplifted the Qinghai-Tibetan Plateau to >3000 m a. s. l. and initialized the glaciations in China [3,4]. Currently, five major glaciations (Xixiabangma, Nyanyaxungla, Zhonglianggao, Guxiang, and the last glaciation) have been recognized to have occurred in the montane regions of western China during the Pleistocene [5,6], but no continuous ice sheet was present [7] and environmental diversity of the tropics and subtropics in lower elevations was still maintained [8]. Many phylogeographic studies have recently explored the evolutionary consequences of climatic fluctuations and the complex local topography in China. Most of these studies focused on the Qinghai-Tibetan Plateau and its surrounding area (e.g. [9]) and southern (e.g. [10]) and eastern

China (e.g. [11]), but less attention has been devoted to southwestern China.

Yunnan is an ideal region to study ecology, distribution and evolution, especially historical geological events, climate oscillations and biological adaptations. Being characterized by dramatic variations in climate and topography, the montane regions of Yunnan support a wide array of habitats. Moreover, during the Quaternary, there was no large-scale continental glaciation in this region [12]. This, combined with a complex, microhabitat-rich topography, would allow species to survive in different refugia and promote intra-specific divergences in small and isolated populations [13].

However, the mechanisms that shape the current genetic structure in Yunnan are still poorly understood, because different species may have different evolutionary trajectories and different response mechanisms to the same historical events. Some studies revealed that lineage divergence times were much earlier than the Pleistocene and genetic structures were shaped by orogenic events [14,15] or historical drainage rearrangements [16–18], and deep river valleys had acted as barriers to gene flow [15,19]. However, other studies revealed that lineage divergences were triggered mainly by climatic oscillations during the Pleistocene [19–21],

although past geologic events had also played an occasional role [21]; and historical or contemporary drainage systems did not contribute to current genetic structure [20,21] (but see [19]). The population structure of a species can be affected by its life history and ecological traits [22], and even sympatric species may have different phylogeographic patterns and genetic structures due to different habitat preferences [21,23]. Thus, more work is needed to investigate the mechanisms shaping the phylogeographic patterns and genetic structures of species in this region from a comparative phylogeographic perspective.

In addition, an accurate delimitation of glacial refugia is a high priority for conservation because these are key areas for the persistence and evolution of biodiversity [24]. The topographically complex region of Yunnan likely provided stable habitats for the survival of species in different refugia during the ice ages, corresponding to the hypothesis of 'refugia within refugia' [25]. A recent study based on plant endemism in China has recognized southern Yunnan as a former glacial refugium [24], and molecular evidence for refugial survival in northwestern Yunnan Plateau has also been recently reported by Zhan et al. [20] and Li et al. [21]. However, up until now only a few studies tried to locate refugia [20,21]. The sparse literature on this region limits our understanding of the development and sustainment of high diversity within the complicated topography of Yunnan.

Amphibians, being terrestrial poikilotherms with narrow habitat requirements and limited dispersal potentials, are useful model animals for population genetic studies. The range of Red Knobby Newt (*Tylotriton shanjing*) spans the Yunnan province of China, from the tropical south, through the subtropical center and west, to the temperate northwest [26,27]. It inhabits moist, vegetated areas close to standing water bodies at elevations of 1000–2100 m [28].

In this study, we examine the evolutionary history of *T. shanjing* to test hypotheses involving the following questions: (i) How did climatic changes during the Pleistocene affect the observed phylogeographic structure and demographic dynamics? (ii) Did historical or contemporary drainage systems contribute to the current patterns of genetic variation? Such information will improve our understanding of the historical and ongoing evolutionary driving forces for maintaining the extraordinarily high biodiversity of Yunnan, China.

Methods

Ethics Statement

All animal samples were collected following the regulations for the implementation of People's Republic of China on the protection of terrestrial wildlife (State Council Decree [1992] No. 13) and approved by Wildlife Protection Office, the Forestry Department of Yunnan Province as well as the Ethics Committee of Kunming Institute of Zoology, Chinese Academy of Sciences.

Sample Collection, DNA Extraction, Amplification and Sequencing

A total of 146 individuals were sampled from 19 populations throughout the entire geographical range of *T. shanjing* (Table 1 and Figure 1). Animals were caught by hand and were sacrificed by diethyl ether anesthesia, and then liver tissues were collected and stored in 99% ethanol immediately after removal. Specimens were fixed in 10% formalin and finally preserved in 70% ethanol. Three congeneric species, *Tylotriton taliangensis*, *Tylotriton kweichowensis*, and *Tylotriton wenxianensis*, were selected as outgroup. Sequences of *T. wenxianensis* were obtained from GenBank (EU880341).

Genomic DNA was extracted from liver tissue fixed in 99% ethanol. Tissue samples were digested using proteinase K, and subsequently purified following a standard phenol/chloroform isolation and ethanol precipitation. Fragments of cytochrome *b* (cyt *b*), control region (CR), tRNA-Phe, and 12S rRNA genes were amplified and sequenced. The cyt *b* fragment was amplified using primers MVZ15 and MVZ16 [29], and a fragment spanning the entire CR, tRNA-Phe and part of the 12S rRNA genes was amplified using primers PRO (D. Buckley, unpublished data; personal communication) and 12SH1478 [30]. PCR amplifications were performed in 50 μ l reactions using the following cycling conditions: an initial denaturing step at 94°C for 5 min; 35 cycles of denaturing at 94°C for 1 min, annealing at 46 (for cyt *b*) or 50°C (for the fragment spanning CR, tRNA-Phe, and 12S rRNA) for 30 s, and one minute extension at 72°C, followed by a final extension step at 72°C for 5 min. PCR products were purified via spin columns. Sequencing of cyt *b* was performed directly using the corresponding PCR primers. For sequencing the fragment spanning CR, tRNA-Phe, and 12S rRNA, the corresponding PCR primers and four internal primers designed by this study were used (Table S1). DNA sequences of both strands were obtained using the BigDye Terminator 3.1 on an ABI PRISM 3730 following the manufacture's instructions.

Phylogenetic Analyses

DNA sequences were aligned using SEQUENCE NAVIGATOR (Applied Biosystems) and rechecked by eye. Haplotypes were identified using DnaSP 5.0 [31]. Maximum parsimony (MP) analysis was performed in PAUP* 4.0B10 [32] using a heuristic search with 1000 random-addition sequence replicates and support for nodes of the resulting MP tree was assessed by analyses of 1000 bootstrap replicates. Bayesian inference (BI) analysis was conducted in MrBayes 3.1.2 [33] based on the best-fit substitution model selected by Modeltest 3.7 [34], and two runs were performed simultaneously with four Markov chains starting from random trees. The Markov chains were run for 2×10^9 generations and sampled every 100 generations. Convergence was confirmed by plots of Ln *L* scores and low standard deviation of split frequencies. The first 2×10^5 generations were discarded as burn-in, and the remaining trees were used to create a 50% majority-rule consensus tree and to estimate Bayesian posterior probabilities.

Estimating Divergence Times

Time to the most recent common ancestor (TMRCA) was estimated using an uncorrelated lognormal relaxed molecular clock model as implemented in BEAST 1.6.2 [35]. To calibrate the rate of divergence, a closest external calibration point was incorporated based on the assumption that divergence between *Pleurodeles waltl* from Iberia and *Pleurodeles poireti* from northern Africa was initiated by a vicariance event at the end of the Messinian salinity crisis, approximately 5.3 Mya [36–39]. We did not use other known fossil records within Salamandridae as calibration because they are more external than the divergence between *P. waltl* and *P. poireti* based on Vicités et al. [40], which will lead to overestimation of times to divergence according to Ho et al. [41] and Hugall et al. [42]. Four independent runs were conducted for 10^7 generations using the HKY+I+G model and sampled every 1000 generations, assuming a coalescent prior of constant population size. These four runs were then combined in Tracer 1.4 [43] to visualize the results of each run as well as examine the effective sample size (ESS) for each parameter, following a burn-in of initial 10% cycles. Mean rate was estimated in this analysis.

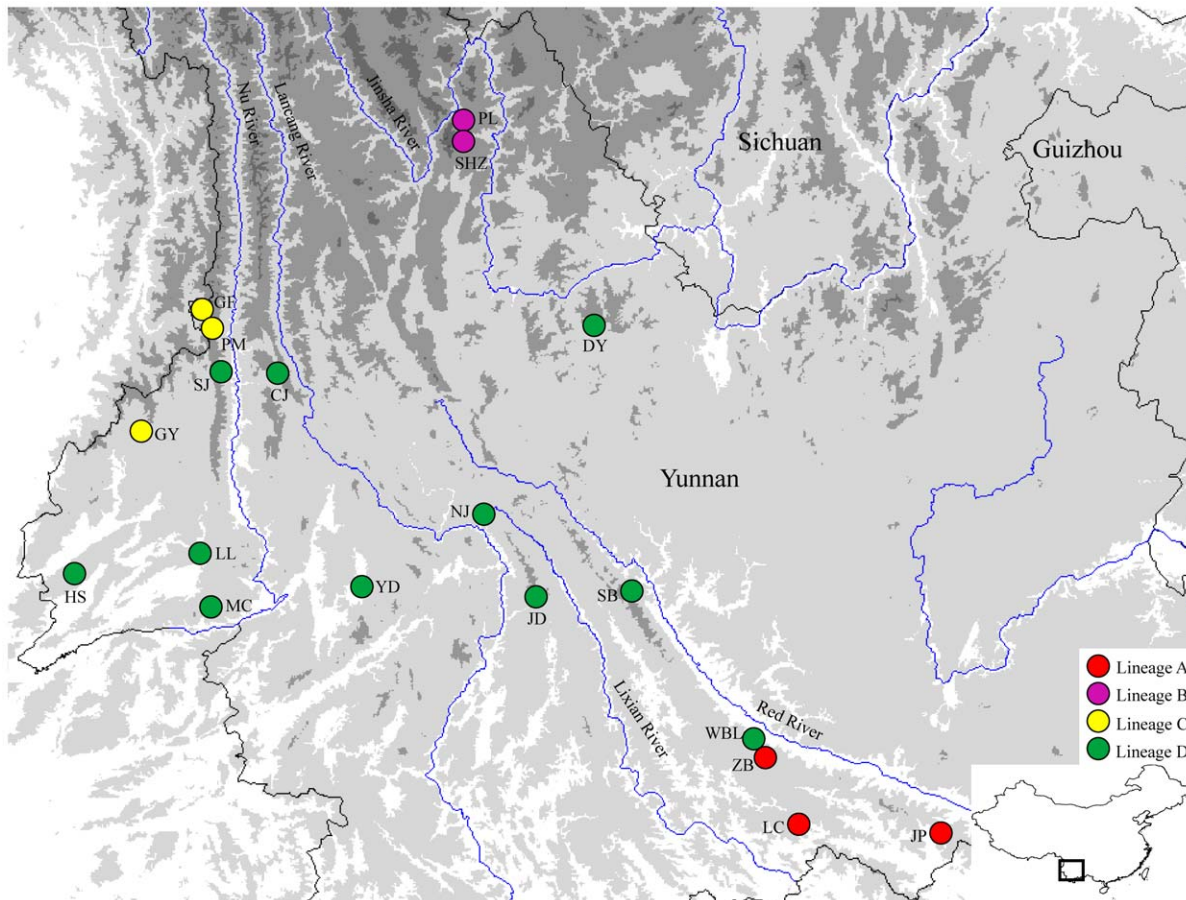


Figure 1. Map showing the sampled populations of *T. shanjing*. Height is reflected by shading and populations are named as in Table 1. doi:10.1371/journal.pone.0056066.g001

Population Analyses

Genetic diversity was estimated by haplotype diversity (h) and nucleotide diversity (π) in Arlequin 3.1 [44]. Three approaches were used to examine geographic partitioning of genetic diversity. First, the haplotype network was estimated using TCS 1.21 [45] based on the 95% parsimony criterion to infer the genealogical relationships among haplotypes. Second, a spatial analysis of molecular variance (SAMOVA) [46] was used to infer population groups. This method uses a simulated annealing procedure to maximize the proportion of total genetic variance due to differences between groups of populations. Third, potential effect of river systems on genetic structure was investigated by analysis of molecular variance (AMOVA) in Arlequin 3.1.

Analysis of Demographic History

Three commonly used methods were applied to examine demographic history. First, we traced population growth using Tajima's D statistics [47] and Fu's F_s test [48] estimated by Arlequin. Significance of D and F_s values were assessed through 1000 simulations. Under demographic expansion, both of these indexes are expected to have significant negative values.

Second, evidence for population expansion was tested by examining pairwise mismatch distributions in Arlequin. Under the null hypothesis of sudden expansion, the raggedness index quantifying the smoothness of the observed mismatch distribution [49] and the sum of squared deviations (SSD) between observed and expected mismatch distribution were computed, and the

statistical significance was tested by P_{Rag} and P_{SSD} , respectively, using a bootstrap approach (1000 replicates). The time at which the population expansion began (t) can be estimated from the relationship $\tau = 2ut$ [50], where τ is the mode of the mismatch distribution and u is the estimated mutation rate of the sequences.

Third, past population dynamics were examined using Bayesian skyline plots [51], a model-free coalescent-based method implemented in BEAST 1.6.2. The mutation rate was fixed to be the mean substitution rate estimated above. Following the HKY+I+G model, 10^7 iterations of the MCMC chains were run, sampling every 1000 iterations and discarding the first 10% as burn-in. Other settings of Bayesian prior were default. Bayesian skyline plots were generated with Tracer 1.4.

Tests of Glacial Refugia Assumptions Based on Coalescent Simulations

Coalescent simulations of genealogies constrained within models of population divergence provide a powerful means of assessing the fit of observed genetic patterns to different phylogeographic hypotheses [52]. To test for the hypothesis that there were multiple glacial refugia rather than a single refugium during Quaternary climatic oscillations, 1000 coalescent genealogies were generated in Mesquite 2.74 [53] under the five historical scenarios of Pleistocene refugia (Figure 2), and the distribution of S , the minimum number of sorting events required to explain population subdivision [54], was recorded. Then, we evaluated model fit by

Table 1. Sampling localities, phylogroup, sample sizes (*N*), haplotypes and their frequencies, gene diversity, nucleotide diversity, and the probability of being the population of origin of the lineage (MRCA %).

Lineage	Population	Haplotypes present (number of individuals)	<i>N</i>	Haplotype diversity	Nucleotide diversity	MRCA %
A	Jinping (JP)	H1 (2), H2 (2), H3 (5), H4 (1)	10	0.7333±0.1199	0.0015±0.0009	35.2
A	Lvchun (LC)	H5 (4), H6 (3), H7 (1), H8 (3), H9 (1)	12	0.8182±0.0703	0.0013±0.0008	63.9
A	Zhangba (ZB)	H10 (1),	1	–	–	1.9
B	Peiliang (PL)	H26 (9), H27 (1)	10	0.2000±0.1541	0.0001±0.0001	43.1
B	Shuanghaizi (SHZ)	H28 (8), H29 (2)	10	0.3556±0.1591	0.0002±0.0002	56.9
C	Gangfang (GF)	H43 (5), H44 (2), H45 (1)	8	0.6071±0.1640	0.0004±0.0004	7.46
C	Pianma (PM)	H43 (7), H45 (5), H46 (2)	14	0.6484±0.0813	0.0004±0.0003	46.07
C	Guyong (GY)	H55 (1)	1	–	–	46.47
D	Wubulu (WBL)	H11 (1), H12 (3)	4	0.5000±0.2652	0.0006±0.0006	16.334
D	Shuangbai (SB)	H13 (10), H14 (2), H15 (1)	13	0.4103±0.1539	0.0002±0.0002	3.03
D	Jingdong (JD)	H13 (7), H16 (1), H17 (1), H18 (1)	10	0.5333±0.1801	0.0020±0.0012	3.314
D	Nanjian (NJ)	H19 (1)	1	–	–	0.352
D	Dayao (DY)	H13 (4), H20 (1), H21 (3), H22 (1), H23 (3), H24 (1), H25 (1)	14	0.8681±0.0594	0.0019±0.0011	15.754
D	Yongde (YD)	H30 (2), H31 (5), H32 (1), H33 (3), H34 (1), H35 (1)	13	0.8205±0.0817	0.0018±0.0011	13.144
D	Caojian (CJ)	H36 (1), H37 (1), H38 (1), H39 (1), H40 (1)	5	1.0000±0.1265	0.0021±0.0014	0.686
D	Shangjiang (SJ)	H41 (3), H42 (1)	4	0.5000±0.2652	0.0008±0.0007	0.078
D	Longling (LL)	H47 (2), H48 (2), H49 (1), H50 (2), H51 (3), H52 (1), H53 (1), H54 (1)	13	0.9231±0.0500	0.0021±0.0012	21.32
D	Mucheng (MC)	H56 (1), H57 (1)	2	1.0000±0.5000	0.0017±0.0019	21.34
D	Husa (HS)	H58 (1)	1	–	–	4.646
Total			146	0.9608±0.0078	0.0097±0.0048	

doi:10.1371/journal.pone.0056066.t001

comparing the *S*-value of the BI genealogy and the *S*-values of the simulated genealogies.

Effective population size (N_e) for the simulations was estimated using the mutation parameter θ (*Theta-W*) calculated by DnaSP. We converted the theta to N_e using the equation $\theta = 2N_e\mu$, with the estimated mean substitution rate. During coalescent simulations, the overall N_e was set to equal the empirical estimate, and the N_e of the refugial population was constrained to a size proportional to the overall N_e . Absolute time (years) was converted to coalescent time (generations), assuming a generation time of 4 years. TMRCA dates estimated from BEAST were used to construct hypotheses of more than one refugium (detailed in Results).

Refugia Localization

Following Dépraz et al. [55], refugia localization reconstruction (RLR) was used to locate refugia for each major group. From the individual-based Bayesian skyline plot analysis (see above), we randomly selected for each clade 500 genealogies from the post-burnin sample using the program RT.PY [56]. Then we treated the sampling locality as a character of the individual and reconstructed the state of the 'locality' character for each node in an unordered parsimonious fashion in Mesquite 2.74.

The number of times that each sampling site was inferred as the unique origin of the root was added over the 500 genealogies. When several *n* localities were equally likely as the common ancestor location, $1/n$ was added to the final score of each sampling site. Then the final sum was divided by the number of genealogies checked (500 here) to give a relative probability score for each locality of having harboured the MRCA of the clade.

Results

Sequence Characteristics

The aligned sequences of *cyt b*, CR, tRNA-Phe, and 12S rRNA were 753, 734, 69, and 817 bp in length, respectively. No insertions or deletions were observed for the protein-coding *cyt b* sequences. Among the 146 individuals, a total of 58 haplotypes were identified by 144 polymorphic sites when all fragments were combined. Sequences of these haplotypes and that of outgroup have been deposited in GenBank under accession numbers JX854457–JX854515, JX854517.

Phylogeny and Divergence Time

The HKY+G+I model was selected as the best-fit model of nucleotide substitution. MP and BI analyses obtained consistent tree topologies (Figure 3). Monophyly of the 58 haplotypes was strongly supported and four major lineages were recognized (A–D), with two of these (C and D) being further subdivided into two sub-lineages (C1 and C2, D1 and D2). Lineage A was restricted to southern Yunnan, lineage B was restricted to northwestern Yunnan, lineage C was restricted to the border region of western Yunnan with Myanmar, and lineage D was comprised of haplotypes from the middle-western Yunnan. In all cases, lineage D was the sister group to the clade of lineages B and C, and A was the sister group to the clade (D, (B, C)).

The divergence time of lineage A from all other lineages was estimated to be approximately 0.83 Mya (95% HPD: 0.46–1.56; Figure 4a). Subsequently, lineage D separated from lineages B and C approximately 0.76 Mya (95% HPD: 0.43–1.43), and lineage B separated from lineage C approximately 0.71 Mya (95% HPD: 0.36–1.28).

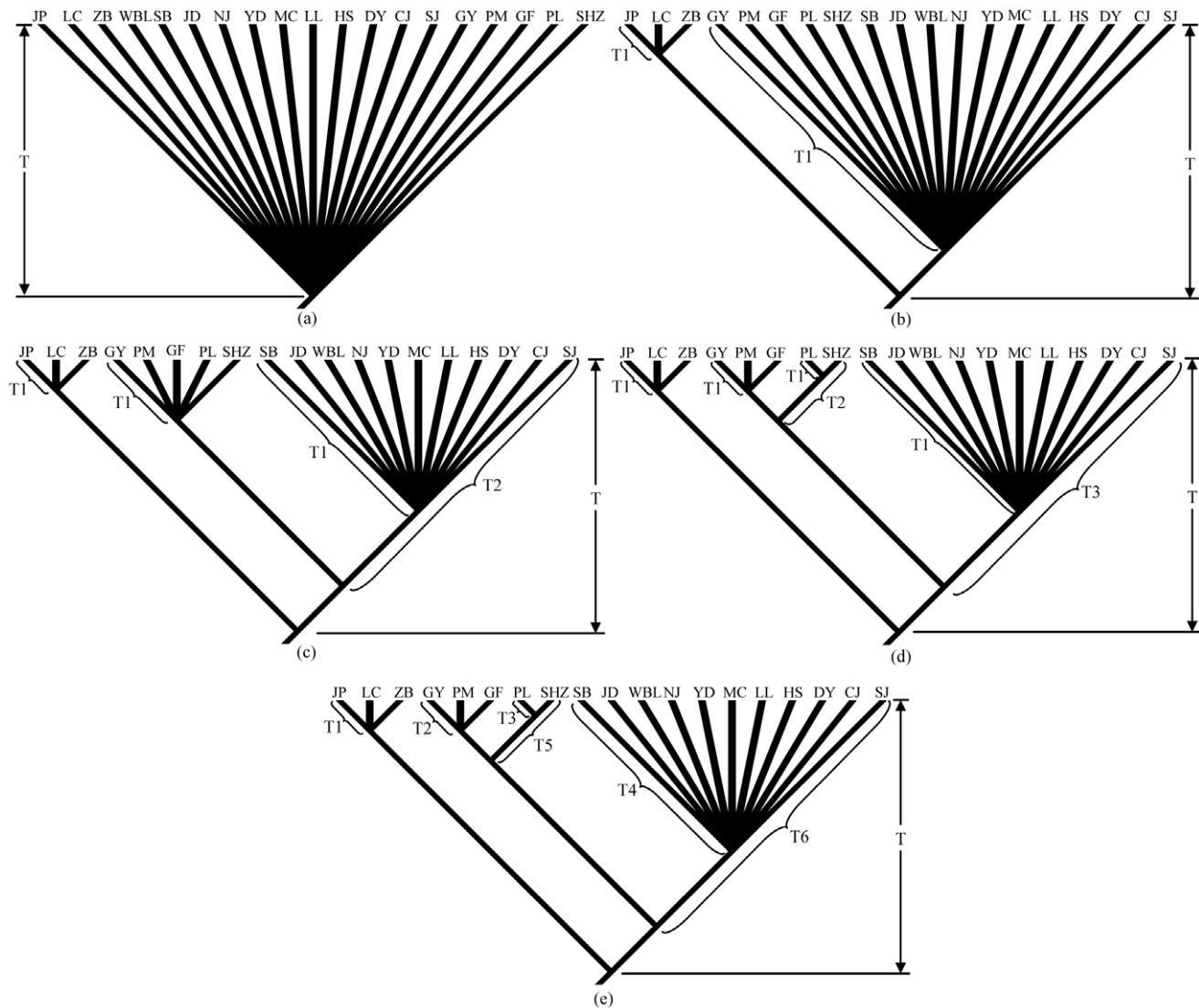


Figure 2. Models of coalescent simulation used to test refugial hypotheses. (a) Hypothesis of single refugium at the end of the Last Glacial Maximum ($T = 18\,000$ years BP); (b) Hypothesis of two refugia at the end of the Last Glacial Maximum ($T_1 = 18\,000$ years BP, $T = 830\,000$ years BP); (c) Hypothesis of three refugia at the end of the Last Glacial Maximum ($T_1 = 18\,000$ years BP, $T_2 = 760\,000$ years BP, $T = 830\,000$ years BP); (d) Hypothesis of four refugia at the end of the Last Glacial Maximum ($T_1 = 18\,000$ years BP, $T_2 = 710\,000$ years BP, $T_3 = 760\,000$ years BP, $T = 830\,000$ years BP); (e) Hypothesis of four refugia before the Last Glacial Maximum ($T_1 = 250\,000$ years BP, $T_2 = 290\,000$ years BP, $T_3 = 70\,000$ years BP, $T_4 = 530\,000$ years BP, $T_5 = 710\,000$ years BP, $T_6 = 760\,000$ years BP, $T = 830\,000$ years BP). The detail interpretation for these models is given in the text. doi:10.1371/journal.pone.0056066.g002

Population Structure

TCS analysis obtained four haplotype networks at 95% probability (connection limit = 21), being consistent with the four major lineages obtained by the phylogenetic analyses (Figure S1). SAMOVA produced similar significant Φ_{CT} values when the numbers of population groups were assumed to be from four to seven (Table 2). Although populations grouped in lineage D are separated by Nu River, Langcang River, Lixian River, and Red River (Figure 1), AMOVA revealed that the values of Φ_{CT} are not significant ($P > 0.05$) and genetic variations among population within groups and within populations are obviously higher than variation among groups when they were partitioned into three or five groups according to the river systems (Table 2), indicating that the river systems had no effect on the genetic structure of these populations.

Demography

For lineage D, neutrality tests obtained significantly negative values ($P < 0.05$, Table 3) and the mismatch analysis obtained a unimodal curve with non-significant values of SSD and raggedness index ($P > 0.05$, Table 3), suggesting that this lineage has undergone population expansions. Considering that lineage D was obviously structured (D1 and D2) and sub-lineage D1 only comprised two individuals from population MC, we further performed analyses only based on sub-lineage D2 and all analyses also supported the hypothesis of expansion. Based on the estimated mean rate of 1.086% substitutions per site per million years, the expansion time of D2 was estimated to be approximately 0.13 Mya, being slightly higher than the estimation from whole lineage of D (Table 3), and the Bayesian skyline plot showed that the N_e of sub-lineage D2 had a trend towards growth from about 0.175 Mya (Figure 5). For lineages

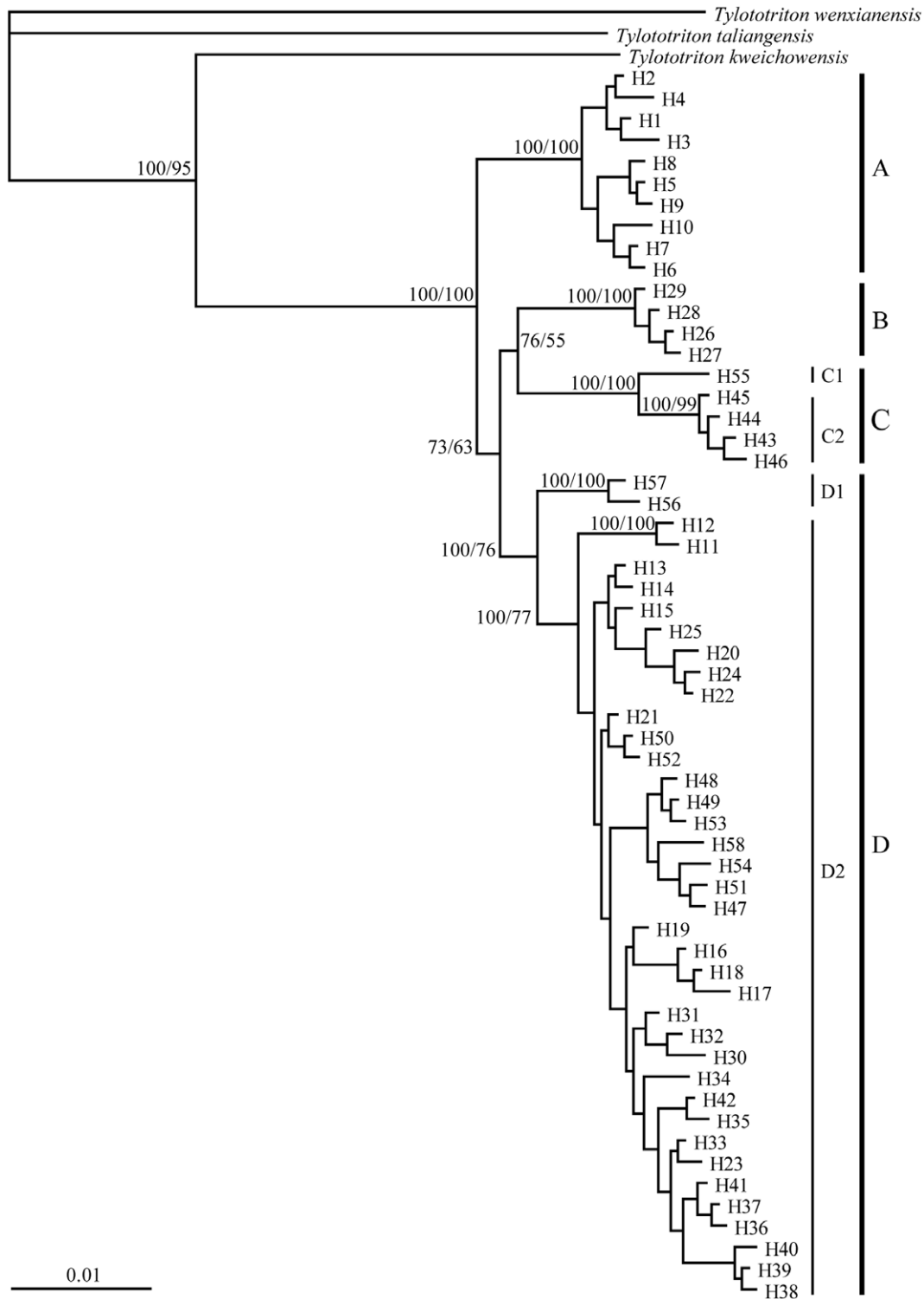


Figure 3. Bayesian inference tree for *T. shanjing* based on the 58 haplotypes from cytochrome *b*, control region, tRNA-Phe, and 12S rRNA sequences. The nodal numbers are BPP and MP bootstrap value, respectively.
doi:10.1371/journal.pone.0056066.g003

A, B, C, and sub-lineage C2, mismatch analyses did not reject the model of sudden population expansion, but both neutrality tests and Bayesian skyline plots rejected the demographic expansion hypothesis.

Glacial Refugia Test

The effective population size was calculated based on the empirical θ values and the estimated mean rate (Table S2). The following five hypotheses concerning glacial refugia were tested. First, extant populations were derived from a single refugium at

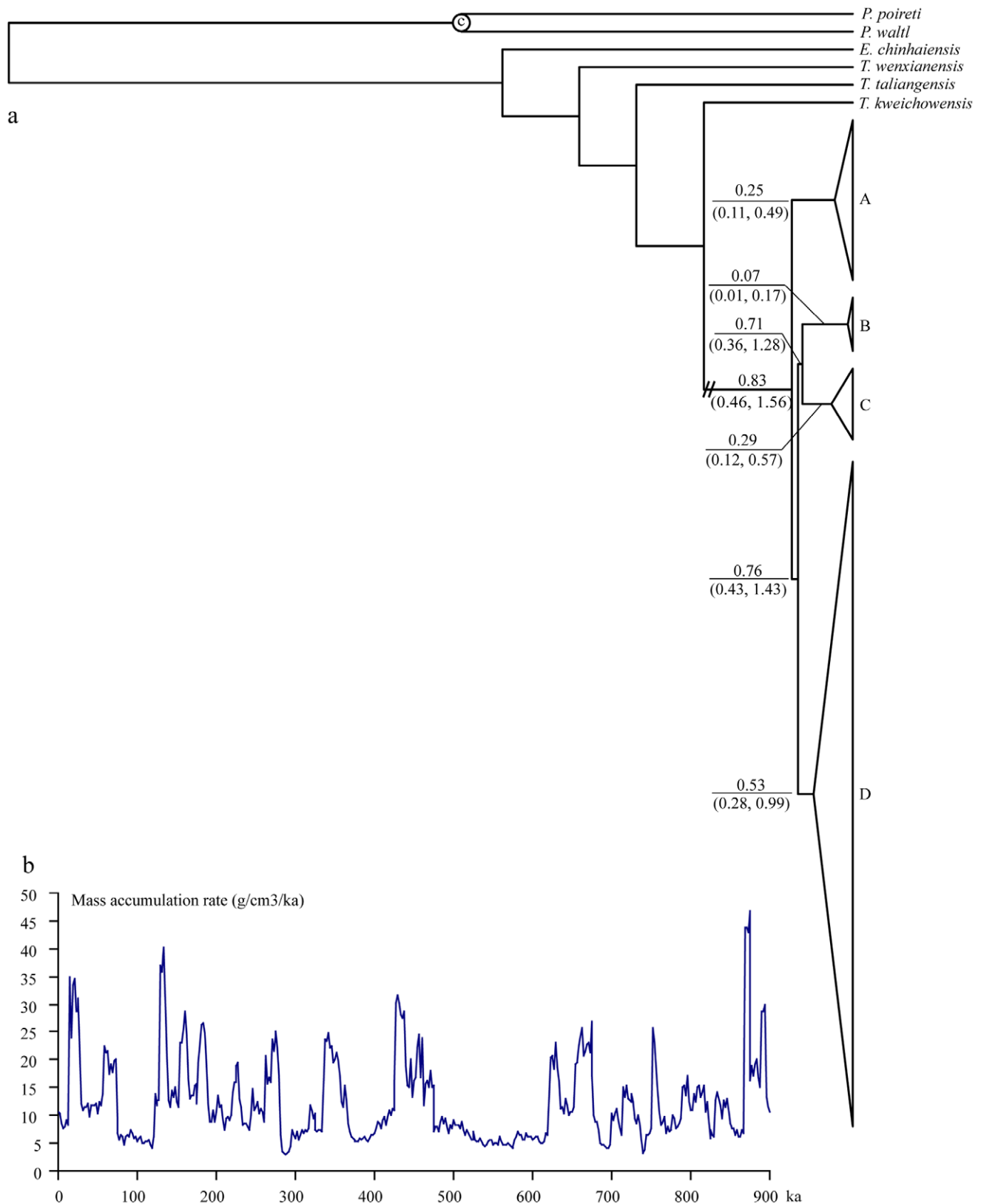


Figure 4. Dated phylogeny and mass accumulation rate of loess. (a) Simplified dated BEAST-derived tree showing divergence dates and TMRCA in Mya with 95% highest probability density (HPD) for major nodes and lineages within *T. shanjing*; (b) Changes in mass accumulation rate of loess deposits on the Chinese Loess Plateau since 0.9 Mya. The data were derived from Sun and An [74].
doi:10.1371/journal.pone.0056066.g004

Table 2. The results of SAMOVA for grouping of all populations and AMOVA for grouping of populations within lineage D.

Grouping option	Φ_{ST}	Φ_{SC}	Φ_{CT}	Among groups	Among population within groups	Within populations
2 groups [JP, LC, ZB, WBL, SB, JD, NJ, DY, PL, SHZ, YD, CJ, SJ, LL, MC, HS] [GF, PM, GY]	0.93097**	0.85584**	0.52115**	52.11%	40.98%	6.9%
3 groups [WBL, SB, JD, NJ, DY, PL, SHZ, YD, CJ, SJ, LL, MC, HS] [JP, LC, ZB] [GF, PM, GY]	0.92294**	0.79623**	0.62184**	62.18%	30.11%	7.71%
4 groups [WBL, SB, JD, NJ, DY, YD, CJ, SJ, LL, MC, HS] [GF, PM, GY] [PL, SHZ] [JP, LC, ZB]	0.91787**	0.60235**	0.79346**	79.35%	12.44%	8.21%
5 groups [PL, SHZ] [GF, PM, GY] [JP, LC, ZB] [WBL] [SB, JD, NJ, DY, YD, CJ, SJ, LL, MC, HS]	0.91562**	0.56252**	0.80712**	80.71%	10.85%	8.44%
6 groups [PL, SHZ] [MC] [GF, PM, GY] [WBL] [JP, LC, ZB] [SB, JD, NJ, DY, YD, CJ, SJ, LL, HS]	0.91466**	0.52669**	0.81970**	81.97%	9.50%	8.53%
7 groups [PL, SHZ] [LC, ZB] [WBL] [SB, JD, NJ, DY, YD, CJ, SJ, LL, HS] [JP] [MC] [GF, PM, GY]	0.91379**	0.49128**	0.83053**	83.05%	8.33%	8.62%
Lineage D: [WBL, SB, JD, NJ, DY, YD, CJ, SJ, LL, MC, HS]	0.54666**				54.67	45.33
Lineage D: [SJ, LL, MC, HS] [CJ, YD] [JD, NJ, SB, WBL, DY]	0.55219**	0.53275**	0.04161*	4.16	51.06	44.78
Lineage D: [SJ, LL, MC, HS] [CJ, YD] [JD, NJ] [SB, WBL] [DY]	0.53320**	0.65529**	-0.35416*	-35.42	88.74	46.68

* $P > 0.05$;** $P < 0.001$.

doi:10.1371/journal.pone.0056066.t002

the end of the Last Glacial Maximum (*c.* 0.018 Mya; Figure 2a). Second, the species survived the Last Glacial Maximum in two refugia isolated *c.* 0.83 Mya (Figure 2b). Third, populations from southern Yunnan diverged from populations from other regions *c.* 0.83 Mya, and populations from middle-western Yunnan were isolated from populations from northwestern Yunnan and the border region of western Yunnan *c.* 0.76 Mya, and then extant populations were derived from three refugia at the end of the Last Glacial Maximum (Figure 2c). Both the fourth and the fifth hypotheses assumed that populations from southern Yunnan diverged from populations from other regions at the middle Pleistocene (*c.* 0.83 Mya), then populations from middle-western Yunnan became isolated from populations from northwestern Yunnan and the border region of western Yunnan (*c.* 0.76 Mya), with populations from northwestern Yunnan and the border region of western Yunnan diverging into two further lineages (*c.* 0.71 Mya; Figure 2d,e). The difference between the fourth and the fifth hypotheses is that the former assumed that extant populations were derived from four refugia at the end of the Last Glacial Maximum (Figure 2d), whereas the latter assumed that extant populations were derived from four refugia before the Last Glacial Maximum based on the estimated TMRCA (Figure 2e).

We calculated $S = 25$ for our BI genealogy. This value does not fall within the 95% confidence interval of the simulated distribution of S for the hypothesis of single refugium, two refugia, three refugia or four refugia at the end of the Last Glacial Maximum but instead falls within the 95% confidence interval of the simulated distribution of S for the hypothesis of four refugia before the Last Glacial Maximum (Figure 6). So we reject the hypotheses of a single refugium, two refugia, three refugia and four refugia at the end of the Last Glacial Maximum in favor of the hypothesis of four refugia before the Last Glacial Maximum.

Discussion

Effect of Drainage System on Genetic Structure

Our data indicate that *T. shanjing* is comprised of four major maternal lineages and the southern lineage (lineage A) is sister to a

clade consisted of the other lineages (Figure 3). The upper Jinsha River drainage originally flowed southward as a tributary to the paleo-Red River [57], under which it could be expected that populations from northwestern Yunnan and the southern Red River drainage area cluster together because they belong to the same paleo-river system. However, in *T. shanjing*, populations from the southern Red River drainage area (lineage A) do not cluster together with populations from northwestern Yunnan (lineage B) (Figure 3). This finding is not compatible with the expectation mentioned above, suggesting that the genetic structure of *T. shanjing* was not shaped by the paleo-river system. Recently, genetic structure of Yunnan pond frog (*Babina pleuraden*) was also found to be not shaped by the paleo-river system [21], but the expected pattern of genetic variation was observed in Yunnan spiny frog (*Nanorana yunnanensis*) [16] and a tree species *Terminalia franchetii* [17,18]. Variations in ecological adaptations affect geographical patterns of genetic variation [58,59]. Both *T. shanjing* and *B. pleuraden* live in lentic environments, whereas *N. yunnanensis* and *T. franchetii* are associated with lotic environments. It is likely that the paleo-river system had no impact on the genetic structure of species preferring for standing water because standing water bodies can act as barriers to gene flow among populations [21,60]. Conversely, the genetic imprint of a paleo-river system can be traced in species associated with lotic environments because flowing water may significantly contribute to the gene flow among populations through the movement of tadpoles and eggs [61].

Although lineage D is distributed across four large rivers (Figure 1), no effect of large rivers could be detected when genetic variation was partitioned by the contemporary river system (Table 2). The species seems to have expanded across these rivers. Populations DY, SB, and JD are separated by the Red River and Lixian River (Figure 1), but H13, the ancestral haplotype of this clade recognized by the TCS analysis, occurs in these three populations (Table 1), suggesting that the Red River and Lixian River are not dispersal barriers for the species. Probably the populations of SB and JD were derived from DY because DY is inferred as one of the origin localities of lineage D (see below)

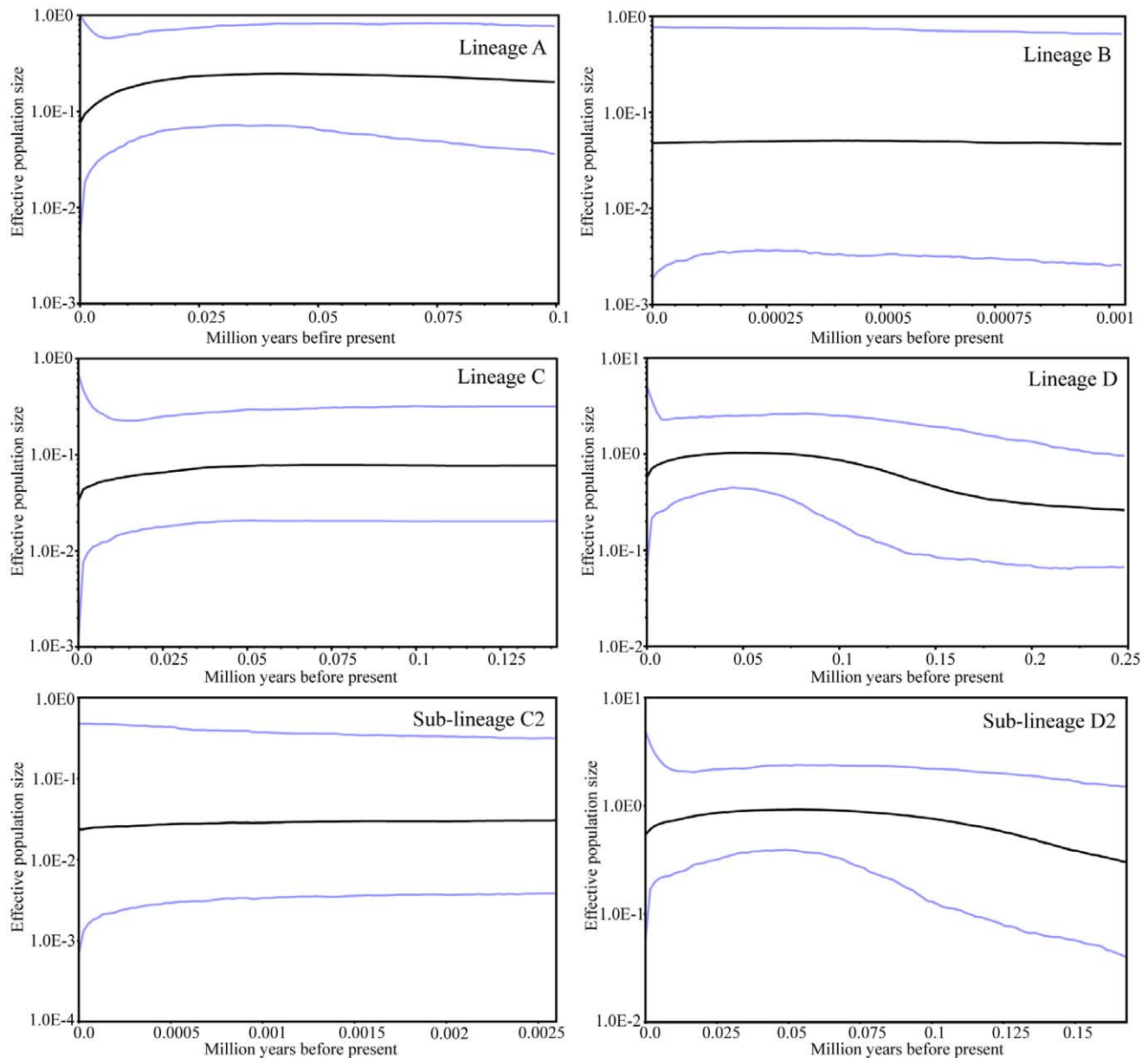


Figure 5. Bayesian skyline plots showing the demographic history of each lineage of *T. shanjing*. Dark lines represent median values for the \log_{10} of the population size, and blue lines represent the 95% highest probability density (HPD) intervals.
doi:10.1371/journal.pone.0056066.g005

Table 3. Results of neutrality tests and mismatch analyses.

Lineage	Neutrality tests		Mismatch distribution			
	Fu's F_s (P -value)	Tajima's D (P -value)	τ	SSD (P_{SSD})	Raggedness (P_{Rag})	Expansion time (Mya)
A	0.639 (0.607)	0.287 (0.647)	9.604	0.021 (0.234)	0.035 (0.344)	–
B	-0.472 (0.317)	-0.094 (0.466)	0.979	0.026 (0.099)	0.184 (0.075)	–
C	1.292 (0.776)	-1.948 (0.015)	1.094	0.006 (0.452)	0.048 (0.839)	–
C2	0.021 (0.479)	0.461 (0.712)	1.053	0.001 (0.711)	0.052 (0.821)	–
D	-16.513 (0.002)	-1.899 (0.010)	6.156	0.003 (0.940)	0.007 (0.932)	0.119
D2	-15.782 (0.000)	-1.796 (0.013)	6.648	0.003 (0.948)	0.007 (0.937)	0.129

doi:10.1371/journal.pone.0056066.t003

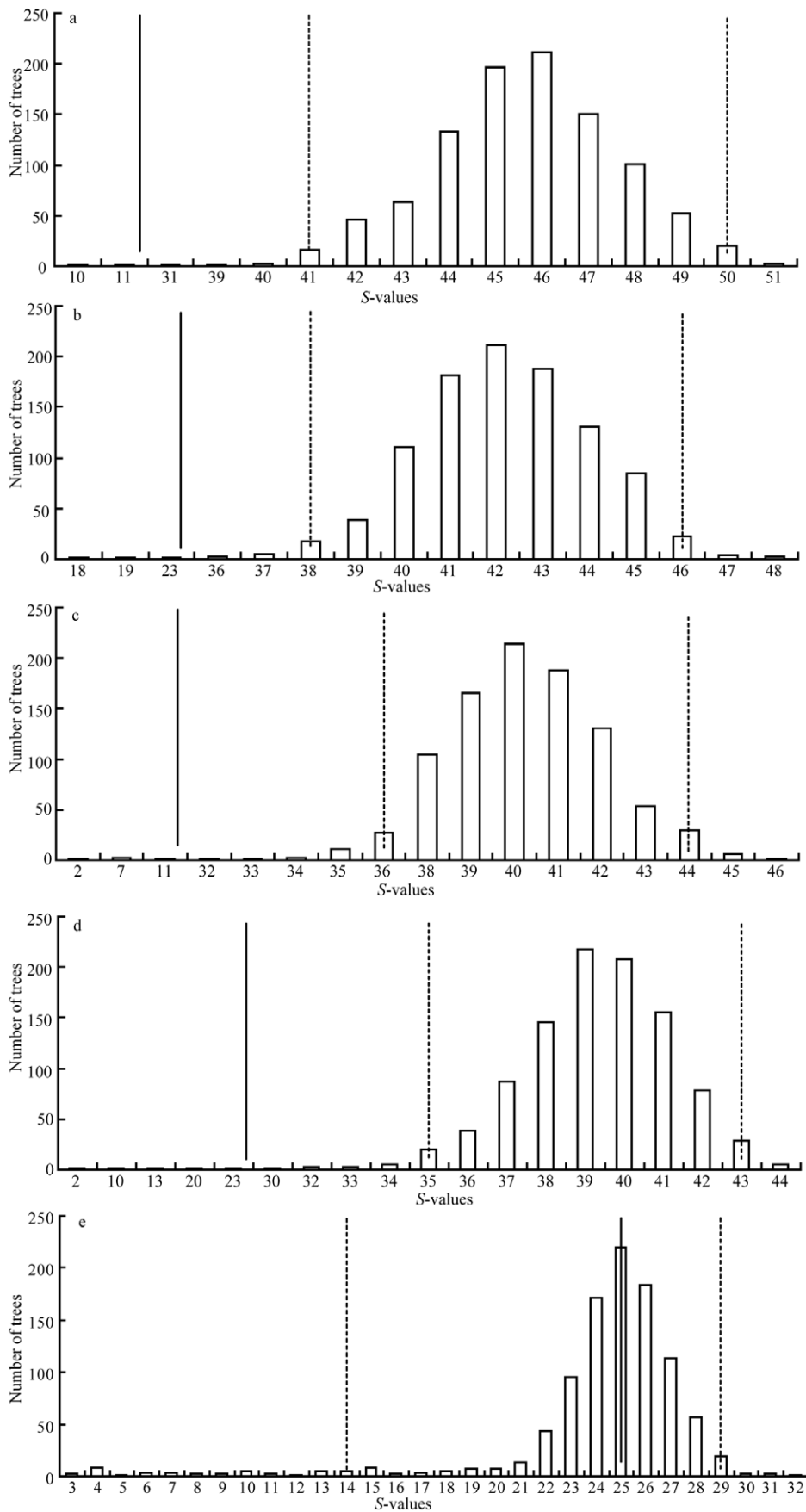


Figure 6. S-values for 1000 simulated coalescent genealogies. (a) Results from simulations within the single refugium hypothesis; (b) Results from simulations within the two refugia hypothesis; (c) Results from simulations within the three refugia hypothesis; (d) Results from simulations within the hypothesis of four refugia at the end of the Last Glacial Maximum; (e) Results from simulations within the hypothesis of four refugia before the Last Glacial Maximum. The black line represents the S-value for BI genealogy and dashed lines represent the 95% credible interval for the distribution.

doi:10.1371/journal.pone.0056066.g006

whereas SB and JD have low relative probability of being the population of origin of the lineage (Table 1).

Lineage Divergence Triggered by Pleistocene Glaciation Events

Geographically no significant east-west barrier exists between the southern lineage (lineage A) and other lineages. The divergence time between the southern lineage and other lineages is estimated to be approximately 0.83 Mya (Figure 4a). This date coincides with a cold stage in the Xixiabangma glaciation (1.17–0.8 Mya; [6]). A high mass accumulation rate for Chinese loess around 0.9 Mya when the glacier expanded extensively [62] supports that it is one of the coldest climatic periods in the region (Figure 4b). Moreover, lineage D diverged from lineages B and C approximately 0.76 Mya, and the timing of the split between lineages B and C is estimated to be approximately 0.71 Mya (Figure 4a). These two divergence events coincide with the Naynayxungla glaciation at 0.78–0.5 Mya, which is the most extensive glaciation occurred during the Middle Pleistocene when there were many large ice caps, glacier complexes and great valley glaciers that covered a total area $\geq 500,000 \text{ km}^2$ [6], and another mass accumulation rate peak of Chinese loess (Figure 4b). Following the advances of these glaciations, lineages within *T. shanjing* became restricted to four different regions that served as refugia with interrupted gene flow. With repeated range size changes, surviving populations have passed through genetic isolation, allowing lineages to diverge [13,59].

The TMRCA of lineages A and C are approximately 0.25 Mya and 0.29 Mya, respectively (Figure 4a). These two dates are consistent with the Guxiang glaciation, the largest glaciation occurred along the southeastern edge of the Tibetan Plateau during Marine Isotope Stages 8–6 [6], and we infer two refugia for *T. shanjing* located in southern Yunnan and the border region of western Yunnan, respectively during this harsh climatic period. Population LC has the highest haplotype diversity among the southern populations and the ancestral haplotype of this group (H5) is present at this site (Table 1), suggesting that this site might have served as the main refugium for lineage A. This is consistent with the analysis of refugia localization, which found that population LC has the highest relative probability of being the population of origin of lineage A (Table 1). For lineage C, the refugium is probably located at PM and GY, which have the highest relative probability of being the populations of origin of this lineage. In addition, the TMRCA of lineages D and B are approximately 0.53 and 0.07 Mya, respectively, being congruent with the Naynayxungla glaciation and the early stage of the last glaciation (0.07–0.01 Mya), respectively. Increased accumulation rates of loess (Figure 4b) supports that the climate became cooler and dryer during these periods. We infer two other refugia for the species during the Naynayxungla glaciation and the early stage of the last glaciation, probably localized to WBL, DY, YD, LL, and MC for lineage D, and SHZ for lineage B (Table 1), although this should be treated with caution because of small sampling size for some populations.

On the basis of our date of the TMRCA for all lineages, it seems that all four refugia were not retained during the Last Glacial Maximum (0.023–0.018 Mya). This is supported by our coalescent

simulation, which rejects the hypotheses of a single refugium, two refugia, three refugia, and four refugia at the end of the Last Glacial Maximum in favor of the hypothesis that current populations were derived from four refugia before the Last Glacial Maximum (Figure 6). Coalescent simulations of Zhan et al. [20] and Li et al. [21] also rejected the hypothesis of single refugium during the Last Glacial Maximum in favor of the hypothesis of multiple refugia for the blood pheasant (*Ithaginis cruentus*) and *B. pleuraden*, respectively. Being consistent with that there was no unified ice-sheet covering the whole plateau throughout the Quaternary glaciations [12], which is a precondition to the existence of multiple refugia, more and more evidence indicates that survival in multiple refugia is relatively common for species in the montane regions in southwestern China (e.g. [10,20,21,63,64]).

Demographic History

Climatic oscillations during the Pleistocene resulted in several glacial-interglacial cycles, which caused expansions and contractions of habitats [59,65]. Among the four major population groups, only lineage D possesses a signal of recent growth (Table 3 and Figure 5). The hypothesis of population expansion was also supported for sub-lineage D2 by all analyses. Although SSD and raggedness index did not reject the null model of population expansion for lineages A, B, and C and sub-lineage C2, these statistics are conservative [66]. Bayesian skyline plot revealed an increasing population size in sub-lineage D2 since *c.* 0.175 Mya and it was estimated to have expanded at about 0.13 Mya by Mismatch analysis. This estimation is earlier than the Last Glacial Maximum, being consistent with most recent studies of species from western China [9,16,20,21] but being different from expansion events after the Last Glacial Maximum in many European and North American species [13,59], reflecting the asynchronicity between glaciations of the montane regions in China and Northern Hemisphere glaciation events [67]. The expansion of sub-lineage D2 is likely to be the consequence of the retreat of the extensive glaciation period (0.5–0.175 Mya; Marine Isotope Stages 12–6) and subsequent warmer and wetter climate during the last inter-glaciation (0.175–0.07 Mya) being equivalent to Marine Isotope Stages 5, as indicated by the decreased mass accumulation rate of loess (Figure 4b). Records of ice core and pollen have indicated a series of warm and humid stages during Marine Isotope Stages 5 [68]. An equivalent expansion time was also estimated in a montane bird *Garrulax elliotii* by Qu et al. [69]. Likely, the sympatric distribution of lineages D and A at Yuanjiang County is the consequence of the expansion of sub-lineage D2. For sub-lineage D1, more samples will be needed to investigate its demographic history because detecting population demographic size changes can be difficult with small sample sizes [70].

On the other hand, the Bayesian skyline plot revealed a recent decreasing trend in population size in lineage A and sub-lineage D2 since *c.* 0.025 Mya (Figure 5), a time corresponding to the beginning of the Last Glacial Maximum when the climate became cooler and the mass accumulation rate reached a peak (Figure 4b), which is consistent with the expectation that profound ecological upheavals during cooler periods would have reduced population sizes. Glacial advances decrease temperatures while increasing

aridity. Pollen data have revealed that the average annual temperature at that time was about 6°C lower than today [71], and annual precipitation was about 40% of that at present [72]. These changes may have contributed to the declines in population sizes during the Last Glacial Maximum.

Although Bayesian skyline plot also showed a recent decreasing trend in population size since *c.* 0.025 Mya for whole lineage C, this should be treated with caution because lineage C was obviously subdivided and no obvious recent fluctuation in population size was observed for sub-lineage C2 (Figure 5). Moreover, significant negative value of Tajima's *D* statistics based on whole lineage C supported population expansion (Table 3), but Bayesian skyline plot did not demonstrate expansion for whole lineage C (Figure 5) and value of Tajima's *D* is positive for sub-lineage C2 (Table 3), possibly reflecting that population subdivision lowers the power of neutrality tests [73]. So inferences based on a single sub-lineage can better reflect demographic history of lineage C and more samples will be needed to investigate demography of sub-lineage C1.

Conclusions

In summary, *T. shanjing* comprises four maternal lineages and divergences of these lineages were triggered by glaciation events during the Pleistocene. The paleo-drainage system, which shaped the genetic structures of two sympatric species associated with lotic environment, had no contribution to the current genetic structure of this lentic environment dwelling species, implying that phylogeographic studies on species with different life history and ecological traits are necessary to achieve full understanding of historical and ongoing evolutionary driving forces. There were four glacial refugia for *T. shanjing* during Pleistocene climatic oscillations, some of which (e.g. northwestern Yunnan and southern Yunnan) have also been suggested as glacial refugia for other species, meaning that these regions should be important for consideration when developing sound conservation policies in

Yunnan. Population expansion occurred prior to the Last Glacial Maximum while declines of population sizes occurred after the beginning of the Last Glacial Maximum. Considering that this study is based entirely on mitochondrial data, nuclear data will be required to obtain a more comprehensive understanding of phylogeography of *T. shanjing*.

Supporting Information

Figure S1 Networks of the 58 haplotypes from cytochrome *b*, control region, tRNA-Phe, and 12S rRNA sequences of *T. shanjing*.

(TIF)

Table S1 Primers used in this study to amplify and sequence.

(DOC)

Table S2 Estimations of the empirical theta values and effective population size.

(DOC)

Acknowledgments

We are grateful to two anonymous reviewers for their helpful comments on the manuscript. We thank Drs. Pengfei Fan, Qingyong Ni, Guozheng Sun, Bei Huang, and Zhongming Chen for their help with sample collection, Dr. Shunqing Lv for the loan of tissues of *T. taliangensis*, Dr. Kai He for his advice on analyzing data, and Ms. Li Jia for her help with laboratory work. We also thank Dr. Jeffery A. Wilkinson and Kevin Messenger for improving the writing.

Author Contributions

Conceived and designed the experiments: DR JY. Performed the experiments: MZ. Analyzed the data: GY MZ. Contributed reagents/materials/analysis tools: DR JY. Wrote the paper: GY MZ DR JY.

References

- Hewitt GM (1996) Some genetic consequences of ice ages, and their role in divergence and speciation. *Biol J Linn Soc* 58: 247–276.
- Axelrod DL, Al-Shehbaz I, Raven PH (1996) History of the modern flora of China. In: Zhang A, Wu S, editors. *Floristic characteristics and diversity of East Asian plants*. New York: Springer. 43–55.
- Li J, Fang X (1998) Uplift of the Tibetan Plateau and environmental changes. *Chinese Sci Bull* 43: 1569–1574.
- Cui Z, Chen Y, Zhang W, Zhou S, Zhou L, et al. (2011) Research history, glacial chronology and origins of Quaternary glaciations in China. *Quatern Sci* 31: 749–764.
- Shi Y (2002) A suggestion to improve the chronology of Quaternary glaciations in China. *J Glaciol Geocryol* 24: 687–692.
- Zheng B, Xu Q, Shen Y (2002) The relationship between climate change and Quaternary glacial cycles on the Qinghai-Tibetan Plateau: review and speculation. *Quatern Int* 97–98: 93–101.
- Li J, Shu Q, Zhou S, Zhao Z, Zhang J (2004) Review and prospects of Quaternary glacial research in China. *J Glaciol Geocryol* 26: 235–243.
- Zhang R (2002) Geological events and mammalian distribution in China. *Acta Zool Sin* 48: 141–153.
- Qu Y, Lei F, Zhang R, Lu X (2010) Comparative phylogeography of five avian species: implications for Pleistocene evolutionary history in the Qinghai-Tibetan plateau. *Mol Ecol* 19: 338–351.
- Mao X, Zhu G, Zhang S, Rossiter SJ (2010) Pleistocene climatic cycling drives intra-specific diversification in the intermediate horseshoe bat (*Rhinolophus affinis*) in Southern China. *Mol Ecol* 19: 2754–2769.
- Qiu Y, Sun Y, Zhang X, Lee JK, Fu C, et al. (2009) Molecular phylogeography of East Asian *Kivexia* (*Hydrangeaceae*) in relation to Quaternary climate change and landbridge configurations. *New Phytol* 183: 480–495.
- Shi Y, Li J, Li B (1998) Uplift and environmental changes of Qinghai-Tibetan Plateau in the late Cenozoic. Guangzhou: Guangdong Science and Technology Press.
- Hewitt GM (2000) The genetic legacy of the Quaternary ice ages. *Nature* 405: 907–913.
- Yuan Q, Zhang Z, Peng H, Ge S (2008) Chloroplast phylogeography of *Dipentodon* (*Dipentodontaceae*) in southwest China and northern Vietnam. *Mol Ecol* 17: 1054–1065.
- Zhang M, Rao D, Yang J, Yu G, Wilkinson JA (2010) Molecular phylogeography and population structure of a mid-elevation montane frog *Leptobrachium ailaonicum* in a fragmented habitat of southwest China. *Mol Phylogenet Evol* 54: 47–58.
- Zhang D, Chen M, Murphy RW, Che J, Pang J, et al. (2010) Genealogy and palaeodrainage basins in Yunnan Province: phylogeography of the Yunnan spiny frog, *Nanorana yunnanensis* (*Dicroglossidae*). *Mol Ecol* 19: 3406–3420.
- Zhang T, Sun H (2011) Phylogeographic structure of *Terminalia franchetii* (*Combretaceae*) in southwest China and its implications for drainage geological history. *J Plant Res* 124: 63–73.
- Zhang T, Comes HP, Sun H (2011) Chloroplast phylogeography of *Terminalia franchetii* (*Combretaceae*) from the eastern Sino-Himalayan region and its correlation with historical river capture events. *Mol Phylogenet Evol* 60: 1–12.
- Liu Q, Chen P, He K, Kilpatrick CW, Liu S, et al. (2012) Phylogeographic study of *Apodemus ilex* (*Rodentia: Muridae*) in southwest China. *PLoS ONE* 7(2): e31453. doi:10.1371/journal.pone.0031453.
- Zhan X, Zheng Y, Wei F, Bruford MW, Jia C (2011) Molecular evidence for Pleistocene refugia at the eastern edge of the Tibetan Plateau. *Mol Ecol* 20: 3014–3026.
- Li Z, Yu G, Rao D, Yang J (2012) Phylogeography and demographic history of *Babina pleuaden* (*Anura, Ranidae*) in southwestern China. *PLoS ONE* 7(3): e34013. doi:10.1371/journal.pone.0034013.
- Hamrick JL, Godt MJW, Sherman-Broyles SL (1992) Factors influencing levels of genetic diversity in woody plants species. *New Forest* 6: 95–124.
- Michaux JR, Libois R, Filippucci MG (2005) So close and so different: comparative phylogeography of two small mammal species, the yellow-necked fieldmouse (*Apodemus flavicollis*) and the woodmouse (*Apodemus sylvaticus*) in the Western Palearctic region. *Heredity* 94: 52–63.
- López-Pujol J, Zhang F, Sun H, Ying T, Ge S (2011) Centres of plant endemism in China: places for survival or for speciation? *J Biogeogr* 38: 1267–1280.

25. Gómez A, Lunt DH (2007) Refugia within refugia: patterns of phylogeographic concordance in the Iberian Peninsula. In: Weiss S, Ferrand N, editors. *Phylogeography of southern European refugia*. New York: Springer. 155–188.
26. Nussbaum RA, Brodie ED, Yang D (1995) A taxonomic review of *Tylotriton verrucosus* Anderson (Amphibia: Caudata: Salamandridae). *Herpetologica* 51: 257–268.
27. Fei L, Ye C, Jiang J (2010) *Colored Atlas of Chinese Amphibians*. Chengdu: Sichuan Publishing House of Science and Technology.
28. Yang D, Rao D (2008) *Amphibia and Reptilia of Yunnan*. Kunming: Yunnan Science and Technology Press.
29. Moritz C, Schneider CJ, Wake DB (1992) Evolutionary relationships within the *Ensatina eschscholtzii* complex confirm the ring species interpretation. *Syst Biol* 41: 273–291.
30. Kocher TD, Thomas WK, Meyer A, Edwards SV, Pääbo S, et al. (1989) Dynamics of mitochondrial DNA evolution in animals: amplification and sequencing with conserved primers. *Proc Natl Acad Sci USA* 86: 6196–6200.
31. Rozas J, Sanchez-DelBarrio JC, Messeguer X, Rozas R (2003) DnaSP, DNA polymorphism analyses by the coalescent and other methods. *Bioinformatics* 19: 2496–2497.
32. Swofford DL (2002) PAUP*: Phylogenetic Analysis Using Parsimony (*and other Methods), Version 4.0. Sunderland, MA: Sinauer Associates.
33. Huelsenbeck JP, Ronquist F (2001) MrBayes: Bayesian inference of phylogeny. *Bioinformatics* 17: 754–755.
34. Posada D, Crandall KA (1998) MODELTEST: testing the model of DNA substitution. *Bioinformatics* 14: 817–818.
35. Drummond AJ, Rambaut A (2007) BEAST: Bayesian evolutionary analysis by sampling trees. *BMC Evol Biol* 7: 214.
36. Carranza S, Wade E (2004) Taxonomic revision of Algero-Tunisian *Pleurodeles* (Caudata: Salamandridae) using molecular and morphological data. Revalidation of the taxon *Pleurodeles nebulosus* (Guichenot, 1850). *Zootaxa* 488: 1–24.
37. Carranza S, Amat F (2005) Taxonomy, biogeography and evolution of *Euproctus* (Amphibia: Salamandridae), with the resurrection of the genus *Calotriton* and the description of a new endemic species from the Iberian Peninsula. *Zool J Linn Soc* 145: 555–582.
38. Sotiropoulos K, Eleftherakos K, Džukić G, Kalezic ML, Legakis A, et al. (2007) Phylogeny and biogeography of the alpine newt *Mesotriton alpestris* (Salamandridae, Caudata), inferred from mtDNA sequences. *Mol Phylogenet Evol* 45: 211–226.
39. Carranza S, Romano A, Arnold EN, Sotgiu G (2008) Biogeography and evolution of European cave salamanders, *Hydromantes* (Urodela: Plethodontidae), inferred from mtDNA sequences. *J Biogeogr* 35: 724–738.
40. Vieites DR, Nieto-Román S, Wake DB (2009) Reconstruction of the climate envelopes of salamanders and their evolution through time. *Proc Natl Acad Sci USA* 106: 19715–19722.
41. Ho SYW, Saarma U, Barnett R, Haile J, Shapiro B (2008) The effect of inappropriate calibration: three case studies in molecular ecology. *PLoS ONE* 3(2): e1615. doi:10.1371/journal.pone.0001615.
42. Huggall AF, Foster R, Lee MSY (2007) Calibration choice, rate smoothing, and the pattern of tetrapod diversification according to the long nuclear gene RAG-1. *Syst Biol* 56: 543–563.
43. Rambaut A, Drummond AJ (2007) Tracer v.1.4. Available: <http://beast.bio.ed.ac.uk/Tracer>.
44. Excoffier L, Laval G, Schneider S (2005) Arlequin ver.3.0: an integrated software package for population genetics data analysis. *Evol Bioinform Online* 1: 47–50.
45. Clement M, Posada D, Crandall KA (2000) TCS: a computer program to estimate gene genealogies. *Mol Ecol* 9: 1657–1660.
46. Dupanloup I, Schneider S, Excoffier L (2002) A simulated annealing approach to define the genetic structure of populations. *Mol Ecol* 11: 2571–2581.
47. Tajima F (1989) Statistical method for testing the neutral mutation hypothesis by DNA polymorphism. *Genetics* 123: 585–595.
48. Fu Y (1997) Statistical tests of neutrality of mutations against population growth, hitchhiking and background selection. *Genetics* 147: 915–925.
49. Harpending HC (1994) Signature of ancient population growth in a low resolution mitochondrial DNA mismatch distribution. *Hum Biol* 66: 591–600.
50. Rogers AR, Harpending HC (1992) Population growth makes waves in the distribution of pairwise genetic differences. *Mol Biol Evol* 9: 552–569.
51. Drummond A, Rambaut A, Shapiro B, Pybus O (2005) Bayesian coalescent inference of past population dynamics from molecular sequences. *Mol Biol Evol* 22: 1185–1192.
52. Knowles LL (2001) Did the Pleistocene glaciations promote divergence? Tests of explicit refugial models in montane grasshoppers. *Mol Ecol* 10: 691–701.
53. Maddison WP, Maddison DR (2010) Mesquite: a modular system for evolutionary analysis. Version 2.74. Available: <http://mesquiteproject.org>.
54. Slatkin M, Maddison WP (1989) A cladistic measure of gene flow inferred from phylogenies of alleles. *Genetics* 123: 603–613.
55. Dépraz A, Cordellier M, Hausser J, Pfenninger M (2008) Postglacial recolonization at a snail's pace (*Trochulus villosus*): confronting competing refugia hypotheses using model selection. *Mol Ecol* 17: 2449–2462.
56. Kauff F (2002) RT.PY. Available: <http://www.luzonilab.net/downloads>.
57. Clark MK, Schoenbohm LM, Royden LH (2004) Surface uplift, tectonics, and erosion of eastern Tibet from large-scale drainage patterns. *Tectonics* 23: TC1006.
58. Gavrilov S (2003) Perspective: models of speciation: what have we learned in 40 years? *Evolution* 57: 2197–2215.
59. Hewitt GM (2004) Genetic consequences of climatic oscillations in the Quaternary. *Philos Trans R Soc Lond B* 359: 183–195.
60. Monaghan MT, Spaak P, Robinson CT, WardJV (2001) Genetic differentiation of *Baetis alpinus* Pictet (Ephemeroptera: Baetidae) in fragmented alpine streams. *Heredity* 86: 395–403.
61. Measey GJ, Tolley KA (2011) Investigating the cause of the disjunct distribution of *Amietophrynus pantherinus*, the Endangered South African western leopard toad. *Conserv Genet* 12: 61–70.
62. Li J, Fang X, Pan B, Zhao Z, Song Y (2001) Late Cenozoic intensive uplift of Qinghai-Xizang Plateau and its impacts on environments in surrounding area. *Quatern Sci* 21: 381–391.
63. Li S, Yeung CKL, Feinstein J, Han L, Le MH, et al. (2009) Sailing though the late Pleistocene: unusual historical demography of an East Asian endemic, the Chinese Hwamei (*Leucodioptron canorum canorum*), during the last glacial period. *Mol Ecol* 18: 622–633.
64. Gao L, Möller M, Zhang X, Hollingsworth ML, Liu J, et al. (2007) High variation and strong phylogeographic pattern among cpDNA haplotypes in *Taxus wallichiana* (Taxaceae) in China and North Vietnam. *Mol Ecol* 16: 4684–4698.
65. Abbott RJ, Brochmann C (2003) History and evolution of the arctic flora: in the footsteps of Eric Hultén. *Mol Ecol* 12: 299–313.
66. Felsenstein J (1992) Estimating effective population size from samples of sequences: inefficiency of pairwise and segregating sites as compared to phylogenetic estimates. *Genetic Research* 59: 139–147.
67. Zhang W, Cui Z, Li Y (2006) Review of the timing and extent of glaciers during the last glacial cycle in the bordering mountains of Tibet and in East Asia. *Quatern Int* 154–155: 32–43.
68. Shi Y, Li J, Li B, Yao T, Wang S, et al. (1999) Uplift of the Qinghai-Xizang (Tibetan) Plateau and East Asia environmental change during late Cenozoic. *Acta Geograph Sin* 54: 10–20.
69. Qu Y, Luo X, Zhang R, Song G, Zou F, et al. (2011) Lineage diversification and historical demography of a montane bird *Garrulax elliotii* - implications for the Pleistocene evolutionary history of the eastern Himalayas. *BMC Evol Biol* 11: 174.
70. Ramos-Onsins SE, Rozas J (2002) Statistical properties of new neutrality tests against population growth. *Mol Biol Evol* 19: 2092–2100.
71. Tang L, Shen C, Kong Z, Wang F, Liu K (1998) Pollen evidence of climate during the Last Glacial Maximum in eastern Tibetan Plateau. *J Glaciol Geocryol* 20: 133–140.
72. Tang L, Shen C, Liao G, Yu S, Li C (2004) Climate change in southeastern Tibet during the Last Glacial Maximum. *Sci China Ser D* 34: 436–442.
73. Ray N, Gurrat M, Excoffier L (2003) Intra-deme molecular diversity in spatially expanding populations. *Mol Biol Evol* 20: 76–86.
74. Sun Y, An Z (2006) Chinese Loess Plateau mass accumulation rate data. IGBP PAGES/World Data Center for Paleoclimatology. Data Contribution Series # 2006-034. NOAA/NCDC Paleoclimatology Programme, Boulder, CO, USA.